

ACCURATE NUMERICAL SCHEME FOR SINGULARLY PERTURBED TIME DELAYED PARABOLIC DIFFERENTIAL EQUATIONS

N. T. NEGERO^{1*}, G. F. DURESSA², §

ABSTRACT. For the numerical solution of the singularly perturbed parabolic convection-diffusion equation with large time delays, a novel class of fitted operator finite difference method is constructed using the Mickens-type scheme. Since the perturbation parameter is the source for the simultaneous occurrence of time-consuming and high-speed phenomena in physical systems that depend on present and past history, our study here is to capture the effect of the parameter on the boundary layer. The time derivative is suitably replaced by a Crank-Nicolson-based scheme, followed by the spatial derivative, which is replaced by a non-standard fitted operator scheme. First-order error bounds in space and second-order error bounds in time are established to provide numerical results.

Keywords: singular perturbation; large time delay; parabolic convection-diffusion problem; denominator function; uniformly convergent.

AMS Subject Classification: 65M06, 65M12, 65M15.

1. INTRODUCTION

A realistic model with time delay partial differential equations has significantly more complicated dynamics than a model without time delay partial differential equations, because a time delay can cause a stable equilibrium to become unstable. Such type of equation arises frequently in the mathematical modelling of science and engineering. A few classical examples involves, for example, control theory [30], population dynamics [15], immune response [4], and chemical kinetics [7]. A wide range of delay parabolic partial differential equations models can be found in Wu [33]. The occurrence of boundary layer in singular perturbation problem was originated in nineteenth century [31]. The solution to such problems undergoes abrupt changes in narrow regions of the domain due to the multiscale character of the associated perturbation parameter(s) [6, 9]. For the numerical solution of singularly perturbed delay partial differential equations, layers are connected with additional difficulties; besides instabilities of certain discretization methods, high computational costs and insufficient resolution are essentially due to the existence of layers

¹ Department of Mathematics, Wollega University, Nekemte, Ethiopia.

e-mail: natitfa@gmail.com; ORCID: <https://orcid.org/0000-0003-1593-735X>.

* Corresponding author.

² Department of Mathematics, Jimma University, Jimma, Oromia, P.O.Box 378, Ethiopia.

e-mail: gammeeef@gmail.com; ORCID: <https://orcid.org/0000-0003-1889-4690>.

§ Manuscript received: April 30, 2023; accepted: July 17, 2023.

TWMS Journal of Applied and Engineering Mathematics, Vol.14, No.4 © Işık University, Department of Mathematics, 2024; all rights reserved.

[3, 6, 7, 10]. Solutions of time delay differential equations are of immense interest, equally in applications and theory.

Much attention has been paid to delay parabolic differential equations and their numerical approximations. Among the first rigorous numerical treatments of singularly perturbed parabolic delay differential equations with delay is the pioneering work of Ansari *et al.* [1] in which second order singularly perturbed delay parabolic differential equations are approximated by finite differences on piecewise Shishkin meshes. In [18, 19, 20, 21] authors solve convection-diffusion singularly perturbed parabolic problems with two small parameters. In the papers, [2, 5, 8, 12, 13, 14, 27, 28, 29, 32], the authors considered numerical study of one parameter singularly perturbed parabolic convection-diffusion equation with time delay.

Except for the authors in [22, 23, 24, 25, 26] most of the previous works for numerical solution of singularly perturbed delay parabolic partial differential equations of convection-diffusion type have been studied on the ε -uniform convergence of solutions based on fitted mesh, and a few interest has been paid to the construction of fitted operator finite difference methods of solutions. As a result, when the perturbation parameter ε becomes very small, it is critical to improve appropriate numerical techniques to cope with the oscillatory character of the solutions, whose accuracy is independent of the parameter value ε .

In this work, we proposed a numerical scheme using a denominator function. Moreover, the goal of this study is to implement more accurate, stable and uniformly convergent numerical scheme for solving singularly perturbed parabolic convection-diffusion problem having large time delay.

2. PROBLEM FORMULATION

Let $\Omega_x = (0, 1)$, $D = \Omega_x \times (0, T]$, and $\Gamma = \Gamma_l \cup \Gamma_b \cup \Gamma_r$, where Γ_l and Γ_r are the left and the right side of the rectangular domain D corresponding to $x = 0$ and $x = 1$, respectively and $\Gamma_b = [0, 1] \times [-\tau, 0]$. Here in this paper, we consider the following class of second-order singularly perturbed time delayed one-dimensional parabolic convection-diffusion problem:

$$\begin{aligned} \mathcal{L}_{\varepsilon,x}u(x, t) \equiv \frac{\partial u(x, t)}{\partial t} - \varepsilon u_{xx}(x, t) + a(x, t)u_x(x, t) + b(x, t)u(x, t) = \\ - c(x, t)u(x, t - \tau) + f(x, t), \forall (x, t) \in D, \end{aligned} \tag{1}$$

initial condition

$$u(x, t) = \phi_b(x, t), (x, t) \in \Gamma_b, \tag{2}$$

and subject to the boundary condition

$$u(0, t) = \phi_l(t), \Gamma_l = \{(0, t) : 0 \leq t \leq T\}, \tag{3}$$

$$u(1, t) = \phi_r(t), \Gamma_r = \{(1, t) : 0 \leq t \leq T\}. \tag{4}$$

$0 < \varepsilon \ll 1$ is a singular perturbation parameter and $\tau > 0$ represents the delay parameter and the functions $a(x, t), b(x, t), c(x, t), f(x, t)$ on \overline{D} and $\phi_b(x, t), \phi_l(t), \phi_r(t)$ on Γ are sufficiently smooth, bounded functions and independent of ε . For small values of perturbation parameter ($\varepsilon \rightarrow 0$) the solution of the problem typically exhibits layer behavior depending on the sign of the convection term. When $a(x, t) \geq \alpha > 0, b(x, t) \geq \beta > 0, c(x, t) \geq \vartheta > 0, (x, t) \in \overline{D}$, the solutions of (1)-(4) exhibits boundary layer along $x = 1$ (i.e, in the neighborhood of Γ_r).

3. BOUNDS FOR THE SOLUTION OF THE CONTINUOUS PROBLEM

Lemma 3.1 (Continuous maximum principle). *Let $\Psi(x, t) \in C^2(D) \cap C^0(\bar{D})$, with $\mathcal{L}_{\varepsilon, x}\Psi(x, t) \geq 0$ in D and $\Psi(x, t) \geq 0$ for all $(x, t) \in \Gamma$. Then we have $\Psi(x, t) \geq 0$, $\forall(x, t) \in \bar{D}$.*

Proof. Suppose there exists $(x^*, t^*) \in \bar{D}$ be such that $\Psi(x^*, t^*) = \min_{(x, t) \in \bar{D}} \Psi(x, t)$ and suppose that $\Psi(x, t) < 0$ which implies $(x^*, t^*) \notin \Gamma$ as $\Psi(x, t) \geq 0$ on Γ . Then, we have $\Psi_x(x^*, t^*) = \Psi_t(x^*, t^*) = 0$ and $\Psi_{xx}(x^*, t^*) \geq 0$ and thus $\mathcal{L}_{\varepsilon, x}\Psi(x^*, t^*) < 0$ which contradicts the given hypothesis and hence $\Psi(x, t) \geq 0$, $\forall(x, t) \in \bar{D}$. \square

Lemma 3.2. *The solution $u(x, t)$ of the continuous problem (1)-(4) satisfy the following estimate:*

$$|u(x, t) - \phi_b(x, 0)| \leq Ct. \quad (5)$$

Proof. For the proof reader can refer to Das and Natesan [5]. \square

Lemma 3.3 (Uniform stability estimate for continuous problem). *The uniform stability bound on the solution $u(x, t)$ of the continuous problems (1)-(2) satisfy:*

$$\|u\| \leq \beta^{-1} \|\mathcal{L}_{\varepsilon, x}u\| + \max(|\phi_b|, (|\phi_l| + |\phi_r|)).$$

Proof. For the barrier functions $\Psi^\pm(x, t) = \beta^{-1} \|\mathcal{L}_{\varepsilon, x}u\| + \max(|\phi_b|, (|\phi_l| + |\phi_r|)) \pm u(x, t)$, $\forall(x, t) \in \bar{D}$ we have

$$\Psi^\pm(0, t) = \beta^{-1} \|\mathcal{L}_{\varepsilon, x}u\| + \max(\phi_b, \max(\phi_l, \phi_r)) \pm u(0, t) \geq 0,$$

$$\Psi^\pm(1, t) = \beta^{-1} \|\mathcal{L}_{\varepsilon, x}u\| + \max(|\phi_b|, (|\phi_l| + |\phi_r|)) \pm u(1, t) \geq 0,$$

$$\begin{aligned} \mathcal{L}_{\varepsilon, x}\Psi^\pm &= b [\beta^{-1} \|\mathcal{L}_{\varepsilon, x}u\| + \max(|\phi_b|, (|\phi_l| + |\phi_r|))] \pm \mathcal{L}_{\varepsilon, x}u(x, t) \geq \\ &\|\mathcal{L}_{\varepsilon, x}u\| + \beta \max(|\phi_b|, (|\phi_l| + |\phi_r|)) \pm \mathcal{L}_{\varepsilon, x}u(x, t) \geq \|\mathcal{L}_{\varepsilon, x}u\| \pm \|\mathcal{L}_{\varepsilon, x}u(x, t)\| \geq 0. \end{aligned}$$

Thus, by applying the maximum principle we obtain the required result. \square

Lemma 3.4. *The exact solution $u(x, t)$ and its derivatives of problems (1)-(4), satisfy the bound:*

$$\left\| \frac{\partial^{i+j}u}{\partial x^i \partial t^j} \right\|_\infty \leq C (1 + \varepsilon^{-i} \exp(-\alpha(1-x)/\varepsilon)), 0 \leq i + 2j \leq 4, \forall(x, t) \in \bar{D}.$$

Proof. For the proof the Lemma 3.4 refer [5]. \square

4. NUMERICAL SCHEME FORMULATION

4.1. The time semidiscretization. On the time domain $[0, T]$ we introduce the equidistant meshes with uniform step size Δt such that

$$\bar{\Omega}_t^M = \{t_n = n\Delta t, n = 0, 1, \dots, M, \Delta t = T/M\},$$

where $M = T/\Delta t$ is the total number of mesh elements in the domain $[0, T]$. Here, we propose a numerical scheme to solve Equations (1)-(4), which consists of the Crank-Nicolson method for the time derivative. This gives the following system of semi-discretize

problem,

$$\begin{cases} \frac{U^{n+1}(x) - U^n(x)}{\Delta t} - \varepsilon (U_{xx})^{n+1/2}(x) + a^{n+1/2}(x) (U_x)^{n+1/2}(x) + b^{n+1/2}(x) U^{n+1/2}(x) \\ = -c^{n+1/2}(x) U^{n+1/2-s}(x) + f^{n+1/2}(x), \\ U^{n+1}(0) = \phi_l(t_{n+1}), 0 \leq n \leq M, \\ U^{n+1}(1) = \phi_r(t_{n+1}), 0 \leq n \leq M, \\ U^{n+1}(x) = \phi_b(x, t_{n+1}), x \in \Omega_x, -(s+1) \leq n \leq -1, \end{cases} \tag{6}$$

where $U^{n+1}(x)$ is the approximate solution of $u(x, t_{n+1})$ at $(n+1)$ th time level. The above equation (6) can be rewritten in operator form as

$$\begin{cases} \mathcal{L}_{\varepsilon,x}^M U^{n+1}(x) \equiv -\frac{\varepsilon}{2} (U_{xx})^{n+1}(x) + \frac{a^{n+1/2}(x)}{2} (U_x)^{n+1}(x) + \\ \frac{1}{2} \left(\frac{2}{\Delta t} + b^{n+1/2}(x) \right) U^{n+1}(x) = \hat{H}^n(x) \\ U^{n+1}(0) = \phi_l(t_{n+1}), 0 \leq n \leq M, \\ U^{n+1}(1) = \phi_r(t_{n+1}), 0 \leq n \leq M, \\ U^{n+1}(x) = \phi_b(x, t_{n+1}), x \in \Omega_x, -(s+1) \leq n \leq -1, \end{cases} \tag{7}$$

where

$$\hat{H}^n(x) = \begin{cases} \frac{\varepsilon}{2} (U_{xx})^n(x) - \frac{a^{n+1/2}(x)}{2} (U_x)^n(x) - \frac{1}{2} \left(\frac{-2}{\Delta t} + b^{n+1/2}(x) \right) U^n(x) - \\ c^{n+1/2}(x) \phi_b^{n+1/2}(x) + f^{n+1/2}(x), \text{ if } t_n < s, \\ \frac{\varepsilon}{2} (U_{xx})^n(x) - \frac{a^{n+1/2}(x)}{2} (U_x)^n(x) - \frac{1}{2} \left(\frac{-2}{\Delta t} + b^{n+1/2}(x) \right) U^n(x) - \\ c^{n+1/2}(x) U^{n+1/2-s}(x) + f^{n+1/2}(x), \text{ if } t_n \geq s. \end{cases}$$

The semidiscrete difference operator $\mathcal{L}_{\varepsilon,x}^M U^{n+1}(x)$ in Equation (7) satisfies the maximum principle as follows.

Lemma 4.1 (Semi-discrete maximum principle). *Let $\Upsilon^{n+1}(x)$ be a smooth function such that $\Upsilon^{n+1}(0) \geq 0$ and $\Upsilon^{n+1}(1) \geq 0$. Then $\mathcal{L}_{\varepsilon,x}^M \Upsilon^{n+1}(x) \geq 0$ for all $x \in D$, implies that $\Upsilon^{n+1}(x) \geq 0$ for all $x \in \bar{D}$.*

Proof. The proof continue as of Lemma 4.1. □

The local truncation error e_{n+1} of the temporal semi-discretization (7) is given by $U^n(x) - u(x, t_n)$ where $u(x, t_n)$ and $U^n(x)$ are the exact and approximate solution of the problem in (1)-(4) as follows.

Lemma 4.2 (Local error estimate). *Suppose that Lemma 3.4 hold. Then the local error estimate associated to the semi-discretized problem (7) is given by*

$$\|e_{n+1}\|_{\infty} \leq C (\Delta t)^3.$$

Proof. The proof can be done by using the Taylor’s series expansion up to $O((\Delta t)^3)$ such that $u(x, t_{n+1/2}) = u(x, t_n + \Delta t/2)$, $u(x, t_n) = u(x, t_n - \Delta t/2)$ and applying the maximum principle given at Lemma 4.1. For more detail the reader referred to Kumar *et al.* [16]. □

Lemma 4.3 (Global error estimate.). *Under the hypothesis of Lemma 4.2, global error estimate E_n in the temporal direction is given by*

$$\|E_n\|_\infty \leq C (\Delta t)^2$$

where E_n is the global error in the temporal direction at $(n + 1)$ th time level.

Proof. Using local error estimates given in Lemma 4.2, the global error estimate at the $(n + 1)$ th time step is given by

$$\begin{aligned} \|E_n\|_\infty &= \left\| \sum_{k=1}^n e_k \right\|, n \leq \frac{T}{\Delta t} \\ &\leq \|e_1\| + \|e_2\| + \dots + \|e_n\| \\ &\leq C_0 ((n)\Delta t)^2 (\Delta t) \\ &\leq C_0 T (\Delta t)^2, \text{ since } n(\Delta t) \leq T \leq C(\Delta t)^2, C = C_0 T, \end{aligned}$$

where C is constant independent of ε and Δt . □

Lemma 4.4. [8] *The solution $U^n(x)$ of semi-discretized problem (7) and its derivatives satisfies*

$$\left| \frac{d^i U^n(x)}{dx^i} \right| \leq C (1 + \varepsilon^{-i} \exp(-\alpha(1-x)/\varepsilon)), \forall(x) \in \bar{D}, 0 \leq i \leq 4.$$

4.2. Spatial discretization. Consider the semi-discretized problem corresponding to the Equation (6):

$$-\frac{\varepsilon}{2} (U_{xx})^{n+1}(x) + \frac{a^{n+1/2}(x)}{2} (U_x)^{n+1}(x) + \frac{1}{2} \left(\frac{2}{\Delta t} + b^{n+1/2}(x) \right) U^{n+1}(x) = \hat{H}^n(x). \quad (8)$$

Using the homogeneous problems corresponding to (8) with constant coefficients gives

$$-\varepsilon (U_{xx})^{n+1}(x) + \hat{\alpha} (U_x)^{n+1}(x) + \hat{r}^* U^{n+1}(x) = 0 \quad (9)$$

where $\frac{1}{2} \left(\frac{2}{\Delta t} + b^{n+1/2}(x) \right) \geq \hat{r}^* > 0$. From Equation (9) we have two linear independent solutions $\exp(\hat{\lambda}_1 x)$ and $\exp(\hat{\lambda}_2 x)$ such that

$$\hat{\lambda}_{1,2} = \frac{-\hat{\alpha} \pm \sqrt{\hat{\alpha}^2 + 4\varepsilon\hat{r}^*}}{-2\varepsilon}. \quad (10)$$

Now we partitioned spatial domain $[0, 1]$ into N number of mesh elements with a uniform meshes of equal length of h . This gives the spatial mesh

$$\Omega_x^N = \{x_m = mh, m = 1, 2, \dots, N, x_0 = 0, x_N = 1, h = 1/N\},$$

where x_m is nodal points. Let us denote the approximate solution to $u(x, t_n)$ at the grid point x_m by $U_m = c_1 \exp(\hat{\lambda}_1 x_m) + c_2 \exp(\hat{\lambda}_2 x_m)$. Using the method in [17] we have

$$\begin{vmatrix} U_{m-1} & \exp(\hat{\lambda}_1 x_{m-1}) & \exp(\hat{\lambda}_2 x_{m-1}) \\ U_m & \exp(\hat{\lambda}_1 x_m) & \exp(\hat{\lambda}_2 x_m) \\ U_{m+1} & \exp(\hat{\lambda}_1 x_{m+1}) & \exp(\hat{\lambda}_2 x_{m+1}) \end{vmatrix} = 0.$$

Evaluation of the determinant gives:

$$\exp\left(\frac{\hat{\alpha}h}{2\varepsilon}\right)U_{m-1} - 2\cosh\left(\frac{h\sqrt{\hat{\alpha}^2 + 4\varepsilon\hat{r}^*}}{2\varepsilon}\right)U_m + \exp\left(\frac{-\hat{\alpha}h}{2\varepsilon}\right)U_{m+1} = 0, \tag{11}$$

which is an exact difference scheme for (9). With some manipulations (11) yields the following scheme for the non homogeneous problem corresponding to the problem (9)

$$-\varepsilon\frac{U_{m-1}^{n+1} - 2U_m^{n+1} + U_{m+1}^{n+1}}{\frac{h\varepsilon}{\hat{\alpha}}(\exp\left(\frac{h\hat{\alpha}}{\varepsilon}\right) - 1)} + \hat{\alpha}\frac{U_m^{n+1} - U_{m-1}^{n+1}}{h} = \hat{H}_m^{n+1}. \tag{12}$$

According to Mickens [17] we introduce a denominator function that constitutes a general property of the schemes (12). Motivated by (12), the non-standard finite difference scheme for the variable coefficient problem is given by

$$-\frac{\varepsilon}{2}\frac{\delta_x^2 U_m^{n+1}}{\hat{\gamma}^2} + \frac{a_m^{n+1/2}}{2}D_x^- U_m^{n+1} + \frac{1}{2}\left(\frac{2}{\Delta t} + b_m^{n+1/2}\right)U_m^{n+1} = \hat{H}_m^n, \tag{13}$$

where

$$\hat{H}^n(x) = \begin{cases} \frac{\varepsilon}{2}\frac{\delta_x^2 U_m^{n+1}}{\hat{\gamma}^2} - \frac{a_m^{n+1/2}}{2}D_x^- U_m^{n+1} - \frac{1}{2}\left(\frac{-2}{\Delta t} + b_m^{n+1/2}\right)U_m^n - c_m^{n+1/2}\phi_b^{n+1/2}(x_m) \\ \quad + f_m^{n+1/2}, \text{ if } t_n < s, \\ \frac{\varepsilon}{2}\frac{\delta_x^2 U_m^{n+1}}{\hat{\gamma}^2} - \frac{a_m^{n+1/2}}{2}D_x^- U_m^{n+1} - \frac{1}{2}\left(\frac{-2}{\Delta t} + b_m^{n+1/2}\right)U_m^n - c_m^{n+1/2}U_m^{n+1/2-s} \\ \quad + f_m^{n+1/2}, \text{ if } t_n \geq s, \end{cases}$$

with $\delta_x^2 U_m^n = U_{m-1}^n - 2U_m^n + U_{m+1}^n$, $\hat{\gamma}^2 = \frac{h\varepsilon}{a_m}(\exp\left(\frac{ha_m}{\varepsilon}\right) - 1)$, $D_x^- U_m^n = \frac{U_m^n - U_{m-1}^n}{h}$.

Equation (13) can be rewritten as:

$$\begin{cases} \mathcal{L}_{\varepsilon,m}^{N,M}U_m^{n+1} = \hat{H}_m^{n+1}, \\ U^{n+1}(0) = \phi_l(t_{n+1}), 0 \leq n \leq M, \\ U^{n+1}(1) = \phi_r(t_{n+1}), 0 \leq n \leq M, \\ U^{n+1}(x_m) = \phi_b(x_m, t_{n+1}), \\ -(s+1) \leq n \leq -1, x_m \in \bar{\Omega}^N, \end{cases} \tag{14}$$

where

$$\mathcal{L}_{\varepsilon,m}^{N,M}U_m^{n+1} = -\frac{\varepsilon}{2}\frac{\delta_x^2 U_m^{n+1}}{\hat{\gamma}^2} + \frac{a_m^{n+1/2}}{2}D_x^- U_m^{n+1} + \frac{1}{2}\left(\frac{2}{\Delta t} + b_m^n\right)U_m^{n+1}.$$

Lemma 4.5 (Discrete maximum principle). *Let $\Psi^{n+1}(x_m)$ be a mesh function such that $\Psi^{n+1}(x_0) \geq 0$ and $\Psi^{n+1}(x_N) \geq 0$. Then $\mathcal{L}_{\varepsilon,m}^{N,M}\Psi^{n+1}(x_m) \geq 0$ for $1 \leq m \leq N-1$, implies that $\Psi^{n+1}(x_m) \geq 0$ for $0 \leq m \leq N$.*

Proof. The proof is same as Lemma 3.1. □

Lemma 4.6 (Uniform stability estimate). *The solution U_m^{n+1} of the discrete scheme in (14) satisfy the bound*

$$|U_m^{n+1}| \leq \frac{\max\left|\mathcal{L}_{\varepsilon,m}^{N,M}U_m^{n+1}\right|}{r^*} + \max\{|\phi_l(t_{n+1})|, |\phi_r(t_{n+1})|\},$$

Proof. The proof is as of Lemma 3.3. □

Lemma 4.7. For all $k \in \mathbb{Z}^+$ on a fixed number of mesh numbers N , and $\varepsilon \rightarrow 0$, we have

$$\lim_{\varepsilon \rightarrow 0} \max_{1 \leq m \leq N-1} \frac{\exp(-\alpha x_m / \varepsilon)}{\varepsilon^k} = 0 \text{ and}$$

$$\lim_{\varepsilon \rightarrow 0} \max_{1 \leq m \leq N-1} \frac{\exp(-\alpha(1-x_m) / \varepsilon)}{\varepsilon^k} = 0,$$

where $x_m = mh, \forall m = 1, 2, \dots, N-1$.

Proof. The proof is given in [11]. □

5. CONVERGENCE ANALYSIS OF THE METHOD

Next, we consider the semidiscrete problem in Equation (7) and the discrete scheme in (14) to find the truncation error of the spatial direction discretization.

Theorem 5.1 (Error estimate in the spatial direction). *Let $U^{n+1}(x_m)$ be the solution of continuous solution (7) after temporal discretization and U_m^{n+1} be the approximate solutions of (14) after the full discretization. Then, the numerical solution U_m^{n+1} of the problem in (14) satisfies the error bound*

$$|\mathcal{L}_{\varepsilon,m}^{N,M}(U^{n+1}(x_m) - U_m^{n+1})| \leq CN^{-1}$$

Proof. Consider the error bound in the spatial direction

$$\begin{aligned} & \left| \mathcal{L}_{\varepsilon,m}^{N,M}(U^{n+1}(x_m) - U_m^{n+1}) \right| = \\ & \left| -\frac{\varepsilon}{2}(U_{xx})^{n+1}(x_m) + \frac{a^{n+1/2}(x_m)}{2}(U_x)^{n+1}(x_m) - \left\{ -\frac{\varepsilon}{2} \frac{\delta_x^2 U_m^{n+1}}{\gamma^2} + \frac{a_m^{n+1/2}}{2} D_x^- U_m^{n+1} \right\} \right| \\ & = \left| -\frac{\varepsilon}{2} \left((U_{xx})^{n+1}(x_m) - \frac{\delta_x^2 U_m^{n+1}}{\gamma^2} \right) + \frac{a^{n+1/2}(x_m)}{2} \left((U_x)^{n+1}(x_m) - D_x^- U_m^{n+1} \right) \right| \\ & \leq C\varepsilon h^2 (U_{xxx})^{n+1}(x_m) + Ch (U_{xx})^{n+1}(x_m), \\ & \leq C\varepsilon h^2 \left| 1 + \varepsilon^{-4} \exp(-\alpha(1-x_m)) \right| + Ch \left| 1 + \varepsilon^{-2} \exp(-\alpha(1-x_m)) \right|. \end{aligned}$$

Applying the bound given in Lemma 3.4 and Lemma 4.7 gives

$$|\mathcal{L}_{\varepsilon,m}^{N,M}(U^{n+1}(x_m) - U_m^{n+1})| \leq Ch = CN^{-1}$$

□

Theorem 5.2 (Error estimate in the fully discrete scheme). *Let u be the solution of the problem (1)-(4) and U be the numerical solution of (14). For the fully discrete scheme, the following parameter uniform error estimate holds:*

$$\sup_{0 \leq \varepsilon < 1} |u - U| \leq C(N^{-1} + (\Delta t)^2).$$

Proof. Immediate result follows from the combination of temporal error bound (Lemma 4.3) and spatial error bound (Theorem 5.1). □

6. NUMERICAL RESULTS

In this section, we utilize the double mesh technique to calculate the maximum point wise error and rate of convergence because the exact solution to the issues is unknown. The maximum pointwise errors $E_\varepsilon^{N,\Delta t}$ and the corresponding order of convergence $p_\varepsilon^{N,\Delta t}$ are computed as

$$E_\varepsilon^{N,\Delta t} = \max_{m,n} \left| U_{m,n}^{N,\Delta t} - U_{m,n}^{4N, \frac{\Delta t}{2}} \right|,$$

$$p_\varepsilon^{N,\Delta t} = \log_2 \left(\frac{E_\varepsilon^{N,\Delta t}}{E_\varepsilon^{4N, \frac{\Delta t}{2}}} \right)$$

and from these values we obtain the ε -uniform error $E^{N,\Delta t}$ and the corresponding ε -uniform order of convergence $p^{N,\Delta t}$ by:

$$E^{N,\Delta t} = \max_\varepsilon E_\varepsilon^{N,\Delta t} \text{ and } p^{N,\Delta t} = \log_2 \left(\frac{E^{N,\Delta t}}{E^{4N, \frac{\Delta t}{2}}} \right).$$

where $U_{m,n}^{N,\Delta t}$ is the numerical solutions obtained by using N, M mesh intervals in space and time direction, respectively. To compute $U_{m,n}^{2N, \frac{\Delta t}{2}}$ we use $2N$ and $2M$ mesh intervals in spatial and temporal direction, respectively.

Example 6.1. Consider

$$\frac{\partial u}{\partial t} - \varepsilon \frac{\partial^2 u}{\partial x^2} + \frac{(5 - x^2)}{3} \frac{\partial u}{\partial x} + tu(x, t) = -u(x, t - \tau) + t^3 x (1 - x) \sin(\pi x), (x, t) \in (0, 1) \times (0, 2],$$

with

$$\begin{cases} u(0, t) = 0, u(1, t) = 0, t \in (0, 2], \\ u(x, t) = 0, (x, t) \in [0, 1] \times [-\tau, 0]. \end{cases}$$

Example 6.2. Consider

$$\begin{aligned} \frac{\partial u}{\partial t} - \varepsilon \frac{\partial^2 u}{\partial x^2} + (2 - x^2) \frac{\partial u}{\partial x} + (x + 1)(t + 1)u(x, t) \\ = -u(x, t - \tau) + 10t^2 \exp(-t)x(1 - x), \\ (x, t) \in (0, 1) \times (0, 2], \end{aligned}$$

with

$$\begin{cases} u(0, t) = 0, u(1, t) = 0, t \in (0, 2], \\ u(x, t) = 0, (x, t) \in [0, 1] \times [-\tau, 0]. \end{cases}$$

We have illustrated the maximum point wise errors $E_\varepsilon^{N,\Delta t}$ and the corresponding numerical rates of convergence $p_\varepsilon^{N,\Delta t}$ calculated by numerical scheme (14) for Example 6.1 and Example 6.2 in Table 1 and Table 3, respectively. The numerical results presented in Tables 1 and 3 shows the fact that the proposed numerical method is accurate of order $O(N^{-1} + (\Delta t)^2)$ as predicted by the theory. From the Tables 1,2,3 and 4 one can clearly observe the ε -uniform convergence of the proposed scheme (14). Figures 1 and 2 clearly indicate that the boundary layer is located at the right side of the rectangular domain. The two Figures (Figure 1 and Figure 2) shows the effect of perturbation parameter on

TABLE 1. Maximum pointwise errors ($E_\varepsilon^{N,\Delta t}$) and the corresponding rate of convergence ($p_\varepsilon^{N,\Delta t}$) of the scheme (14) for Example 6.1.

$\varepsilon \downarrow$	$N = 16$		$N = 32$		$N = 64$		$N = 128$		$N = 256$	
	$M = 32$	$M = 64$	$M = 64$	$M = 128$	$M = 128$	$M = 256$	$M = 256$	$M = 512$	$M = 512$	$M = 512$
2^{-10}	$8.5794e-03$	$4.7247e-03$	$4.7247e-03$	$2.4842e-03$	$2.4842e-03$	$1.2662e-03$	$1.2662e-03$	$5.7271e-04$	$5.7271e-04$	$5.7271e-04$
	0.86065	0.92744	0.92744	0.97228	0.97228	1.1446	1.1446	-	-	-
2^{-12}	$8.5794e-03$	$4.7247e-03$	$4.7247e-03$	$2.4842e-03$	$2.4842e-03$	$1.2743e-03$	$1.2743e-03$	$6.4503e-04$	$6.4503e-04$	$6.4503e-04$
	0.86065	0.92744	0.92744	0.96308	0.96308	0.98227	0.98227	-	-	-
2^{-14}	$8.5794e-03$	$4.7247e-03$	$4.7247e-03$	$2.4842e-03$	$2.4842e-03$	$1.2743e-03$	$1.2743e-03$	$6.4504e-04$	$6.4504e-04$	$6.4504e-04$
	0.86065	0.92744	0.92744	0.96308	0.96308	0.98224	0.98224	-	-	-
2^{-16}	$8.5794e-03$	$4.7247e-03$	$4.7247e-03$	$2.4842e-03$	$2.4842e-03$	$1.2743e-03$	$1.2743e-03$	$6.4504e-04$	$6.4504e-04$	$6.4504e-04$
	0.86065	0.92744	0.92744	0.96308	0.96308	0.98224	0.98224	-	-	-
2^{-18}	$8.5794e-03$	$4.7247e-03$	$4.7247e-03$	$2.4842e-03$	$2.4842e-03$	$1.2743e-03$	$1.2743e-03$	$6.4504e-04$	$6.4504e-04$	$6.4504e-04$
	0.86065	0.92744	0.92744	0.96308	0.96308	0.98224	0.98224	-	-	-
2^{-20}	$8.5794e-03$	$4.7247e-03$	$4.7247e-03$	$2.4842e-03$	$2.4842e-03$	$1.2743e-03$	$1.2743e-03$	$6.4504e-04$	$6.4504e-04$	$6.4504e-04$
	0.86065	0.92744	0.92744	0.96308	0.96308	0.98224	0.98224	-	-	-
2^{-22}	$8.5794e-03$	$4.7247e-03$	$4.7247e-03$	$2.4842e-03$	$2.4842e-03$	$1.2743e-03$	$1.2743e-03$	$6.4504e-04$	$6.4504e-04$	$6.4504e-04$
	0.86065	0.92744	0.92744	0.96308	0.96308	0.98224	0.98224	-	-	-
2^{-30}	$8.5794e-03$	$4.7247e-03$	$4.7247e-03$	$2.4842e-03$	$2.4842e-03$	$1.2743e-03$	$1.2743e-03$	$6.4504e-04$	$6.4504e-04$	$6.4504e-04$
	0.86065	0.92744	0.92744	0.96308	0.96308	0.98224	0.98224	-	-	-
$E^{N,\Delta t}$	$8.5794e-03$	$4.7247e-03$	$4.7247e-03$	$2.4842e-03$	$2.4842e-03$	$1.2743e-03$	$1.2743e-03$	$6.4504e-04$	$6.4504e-04$	$6.4504e-04$
$p^{N,\Delta t}$	0.86065	0.92744	0.92744	0.96308	0.96308	0.98224	0.98224	-	-	-

TABLE 2. Maximum pointwise errors ($E_\varepsilon^{N,\Delta t}$) and the corresponding rate of convergence ($p_\varepsilon^{N,\Delta t}$) of the scheme (14) for Example 6.1.

$\varepsilon \downarrow$	Number of mesh intervals $N = M$				
	32	64	128	256	512
2^{-10}	$4.1194e-03$	$2.2161e-03$	$1.1402e-03$	$5.1237e-04$	$2.4987e-04$
	0.89441	0.95874	1.1540	1.0360	-
2^{-12}	$4.1194e-03$	$2.2162e-03$	$1.1482e-03$	$5.8424e-04$	$2.9265e-04$
	0.89435	0.94871	0.97474	0.99738	-
2^{-14}	$4.1194e-03$	$2.2162e-03$	$1.1482e-03$	$5.8425e-04$	$2.9470e-04$
	0.89435	0.94871	0.97472	0.98734	-
2^{-16}	$4.1194e-03$	$2.2162e-03$	$1.1482e-03$	$5.8425e-04$	$2.9470e-04$
	0.89435	0.94871	0.97472	0.98734	-
2^{-18}	$4.1194e-03$	$2.2162e-03$	$1.1482e-03$	$5.8425e-04$	$2.9470e-04$
	0.89435	0.94871	0.97472	0.98734	-
2^{-20}	$4.1194e-03$	$2.2162e-03$	$1.1482e-03$	$5.8425e-04$	$2.9470e-04$
	0.89435	0.94871	0.97472	0.98734	-
2^{-22}	$4.1194e-03$	$2.2162e-03$	$1.1482e-03$	$5.8425e-04$	$2.9470e-04$
	0.89435	0.94871	0.97472	0.98734	-
2^{-30}	$4.1194e-03$	$2.2162e-03$	$1.1482e-03$	$5.8425e-04$	$2.9470e-04$
	0.89435	0.94871	0.97472	0.98734	-
$E^{N,\Delta t}$	$4.1194e-03$	$2.2162e-03$	$1.1482e-03$	$5.8425e-04$	$2.9470e-04$
$p^{N,\Delta t}$	0.89435	0.94871	0.97472	0.98734	-

TABLE 3. Maximum pointwise errors ($E_\varepsilon^{N,\Delta t}$) and the corresponding rate of convergence ($p_\varepsilon^{N,\Delta t}$) of the scheme (14) for Example 6.2.

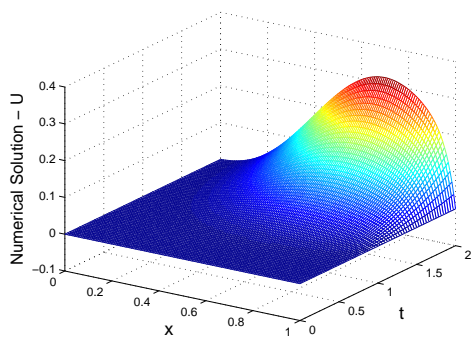
$\varepsilon \downarrow$	N=16	N=32	N=64	N=128	N=256
	M=32	M=64	M=128	M=256	M=512
2^{-10}	$5.7930e-03$	$3.1944e-03$	$1.6717e-03$	$8.6871e-04$	$4.4658e-04$
	0.85877	0.93423	0.94437	0.95996	–
2^{-12}	$5.7930e-03$	$3.1944e-03$	$1.6720e-03$	$8.6885e-04$	$4.4758e-04$
	0.85877	0.93397	0.94440	0.95696	–
2^{-14}	$5.7930e-03$	$3.1944e-03$	$1.6720e-03$	$8.6885e-04$	$4.4813e-04$
	0.85877	0.93397	0.94440	0.95519	–
2^{-16}	$5.7930e-03$	$3.1944e-03$	$1.6720e-03$	$8.6885e-04$	$4.4813e-04$
	0.85877	0.93397	0.94440	0.95519	–
2^{-18}	$5.7930e-03$	$3.1944e-03$	$1.6720e-03$	$8.6885e-04$	$4.4813e-04$
	0.85877	0.93397	0.94440	0.95519	–
2^{-20}	$5.7930e-03$	$3.1944e-03$	$1.6720e-03$	$8.6885e-04$	$4.4813e-04$
	0.85877	0.93397	0.94440	0.95519	–
2^{-22}	$5.7930e-03$	$3.1944e-03$	$1.6720e-03$	$8.6885e-04$	$4.4813e-04$
	0.85877	0.93397	0.94440	0.95519	–
2^{-30}	$5.7930e-03$	$3.1944e-03$	$1.6720e-03$	$8.6885e-04$	$4.4813e-04$
	0.85877	0.93397	0.94440	0.95519	–
$E^{N,\Delta t}$	$5.7930e-03$	$3.1944e-03$	$1.6720e-03$	$8.6885e-04$	$4.4813e-04$
$p^{N,\Delta t}$	0.85877	0.93397	0.94440	0.95519	–

TABLE 4. Maximum pointwise errors ($E_\varepsilon^{N,\Delta t}$) and the corresponding rate of convergence ($p_\varepsilon^{N,\Delta t}$) of the scheme (14) for Example 6.2.

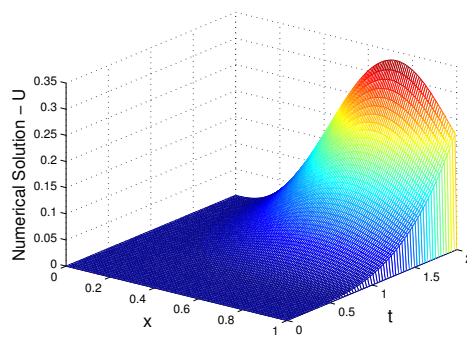
$\varepsilon \downarrow$	Number of mesh intervals $N = M$				
	32	64	128	256	512
2^{-10}	$2.7672e-03$	$1.4555e-03$	$7.2885e-04$	$3.64176e-04$	$1.8146e-04$
	0.92691	0.99782	1.0010	1.0050	–
2^{-12}	$2.7672e-03$	$1.4558e-03$	$7.4606e-04$	$3.7748e-04$	$1.8914e-04$
	0.92661	0.96445	0.98289	0.99695	–
2^{-14}	$2.7672e-03$	$1.4558e-03$	$7.4606e-04$	$3.7757e-04$	$1.8933e-04$
	0.92661	0.96445	0.98255	0.99584	–
2^{-16}	$2.7672e-03$	$1.4558e-03$	$7.4606e-04$	$3.7757e-04$	$1.8933e-04$
	0.92661	0.96445	0.98255	0.99584	–
2^{-18}	$2.7672e-03$	$1.4558e-03$	$7.4606e-04$	$3.7757e-04$	$1.8933e-04$
	0.92661	0.96445	0.98255	0.99584	–
2^{-20}	$2.7672e-03$	$1.4558e-03$	$7.4606e-04$	$3.7757e-04$	$1.8933e-04$
	0.92661	0.96445	0.98255	0.99584	–
2^{-22}	$2.7672e-03$	$1.4558e-03$	$7.4606e-04$	$3.7757e-04$	$1.8933e-04$
	0.92661	0.96445	0.98255	0.99584	–
2^{-30}	$2.7672e-03$	$1.4558e-03$	$7.4606e-04$	$3.7757e-04$	$1.8933e-04$
	0.92661	0.96445	0.98255	0.99584	–
$E^{N,\Delta t}$	$2.7672e-03$	$1.4558e-03$	$7.4606e-04$	$3.7757e-04$	$1.8933e-04$
$p^{N,\Delta t}$	0.92661	0.96445	0.98255	0.99584	–

TABLE 5. Comparison of uniform error ($E^{N,\Delta t}$) and the corresponding uniform rate of convergence ($p^{N,\Delta t}$) for Example 6.2.

Methods↓		$N = 32$	$N = 64$	$N = 128$	$N = 256$
		$M = 40$	$M = 80$	$M = 160$	$M = 320$
Proposed method	$E^{N,\Delta t}$	$2.9360e - 03$	$1.5418e - 03$	$7.8940e - 04$	$3.9932e - 04$
	$p^{N,\Delta t}$	0.92924	0.96579	0.98321	-
Method in [27]	$E^{N,\Delta t}$	$7.8114e - 03$	$4.1163e - 03$	$2.1158e - 03$	$1.0729e - 03$
	$p^{N,\Delta t}$	0.9242	0.9601	0.9797	-
Method in [8]	$E^{N,\Delta t}$	$9.9504e - 03$	$5.8541e - 03$	$3.3439e - 03$	$1.8650e - 03$
	$p^{N,\Delta t}$	0.7653	0.8079	0.8424	-
		$N = 32$	$N = 64$	$N = 128$	$N = 256$
		$M = 30$	$M = 60$	$M = 120$	$M = 240$
Proposed method	$E^{N,\Delta t}$	$2.7115e - 03$	$1.4273e - 03$	$7.3165e - 04$	$3.7034e - 04$
	$p^{N,\Delta t}$	0.92580	0.96406	0.98230	-
Method in [2]	$E^{N,\Delta t}$	$1.0257e - 02$	$5.4993e - 03$	$2.8584e - 03$	$1.4628e - 03$
	$p^{N,\Delta t}$	0.89928	0.94400	0.96647	-

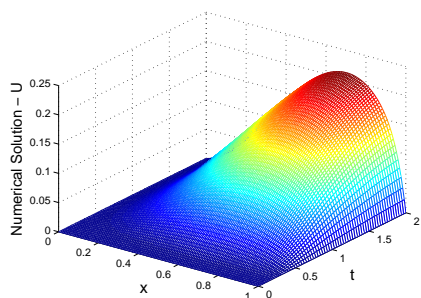


(A)

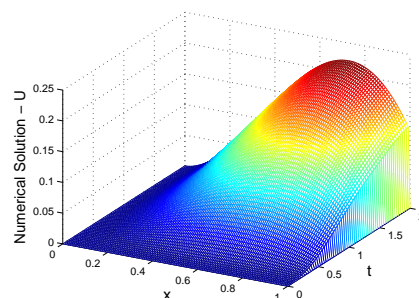


(B)

FIGURE 1. Surface plot of the numerical solution for Example 6.1 with $N = 128, M = 64$, **a** $\varepsilon = 2^{-4}$, **b** $\varepsilon = 2^{-18}$.



(A)



(B)

FIGURE 2. Surface plot of the numerical solution for Example 6.2 with $N = 120, M = 64$, **a** $\varepsilon = 2^{-4}$, **b** $\varepsilon = 2^{-18}$.

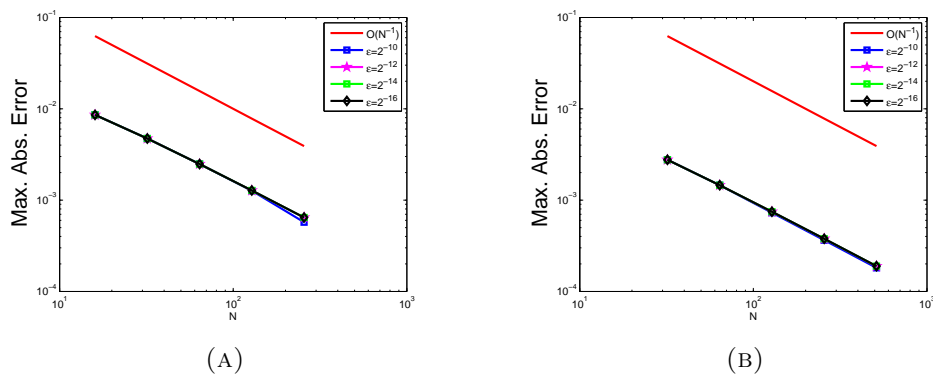


FIGURE 3. Log-Log plot of the maximum error for Example 6.1 on left ([a]) and Example 6.2 on right([b]).

the steepness of layer of the solution. In order to reveal the numerical order of convergence, we have plotted the maximum pointwise errors of Example 6.1 and Example 6.2 in Figure 3 (a) and Figure 3(b), respectively in the log-log scale for which again confirms the effectiveness of the proposed method and also it gives close to first-order.

7. CONCLUSION

In this paper, a singularly perturbed parabolic partial differential equation with a large time delay is considered. Because of the perturbation parameter, the solution of the investigated problem exhibits boundary layer behaviour on the right side of the spatial domain. To obtain parameter-uniform convergence, we have employed the Mickens-type finite difference method for the space discretization and the Crank-Nicolson method for the time discretization, both on a uniform mesh. Thus, the proposed fitted finite difference method converges properly, and the results are better (See Table 5). Theoretically, we have derived that the proposed method provides a first-order in space and second-order in time error estimate. Two numerical experiments are carried out to validate the analytical findings.

Acknowledgement. The authors would like to extend their gratitude to the referees.

REFERENCES

- [1] Ansari A., Bakr S., Shishkin G., (2007), A parameter-robust finite difference method for singularly perturbed delay parabolic partial differential equations, *J. Comput. Appl. Math.*, 205(1), pp. 552–566.
- [2] Babu G., Prithvi M., Sharma K. K., Ramesh V. P., (2022), A robust numerical algorithm on harmonic mesh for parabolic singularly perturbed convection-diffusion problems with time delay, *Numer. Algorithms*, 91(2), pp. 615–634.
- [3] Choudhary M., Kaushik A., (2023), A uniformly convergent defect correction method for parabolic singular perturbation problems with a large delay, *J. Appl. Math. Comput.*, 69(2), pp. 1377–1401.
- [4] Cooke K., Kuang Y., Li B., (1998), Analyses of an antiviral immune response model with time delays, *Canad. Appl. Math. Quart.*, 6(4), pp. 321–354.
- [5] Das A., Natesan S., (2015), Uniformly convergent hybrid numerical scheme for singularly perturbed delay parabolic convection-diffusion problems on Shishkin mesh, *Appl. Math. Comput.*, 271, pp. 168–186.
- [6] Doolan E. P., Miller J. J., Schilders W. H., (1980), *Uniform numerical methods for problems with initial and boundary layers*, Boole Press.
- [7] Epstein I. R., (1992), Delay effects and differential delay equations in chemical kinetics, *Int. Rev. Phys. Chem.*, 11(1), pp. 135–160.

- [8] Gowrisankar S., Natesan S., (2017), ε -uniformly convergent numerical scheme for singularly perturbed delay parabolic partial differential equations, *Int. J. Comput. Math.*, 94(5), pp. 902–921.
- [9] Gupta A., Kaushik A., (2022), A higher-order hybrid finite difference method based on grid equidistribution for fourth-order singularly perturbed differential equations, *J. Appl. Math. Comput.*, 68 (2), pp. 1163–1191.
- [10] Gupta A., Kaushik A., Sharma M., (2023), A higher-order hybrid spline difference method on adaptive mesh for solving singularly perturbed parabolic reaction-diffusion problems with robin-boundary conditions, *Numer. Methods Partial Differ. Equ.*, 39(2), 1220–1250.
- [11] Kadalbajoo M. K., Patidar K. C., Sharma K. K., (2006), ε -uniformly convergent fitted methods for the numerical solution of the problems arising from singularly perturbed general DDEs, *Appl. Math. Comput.*, 182(1), pp. 119–139.
- [12] Kaushik A., Sharma K., Sharma M., (2010), A parameter uniform difference scheme for parabolic partial differential equation with a retarded argument, *Appl. Math. Model.*, 34(12), pp. 4232–4242.
- [13] Kaushik A., Sharma M., (2012), A robust numerical approach for singularly perturbed time delayed parabolic partial differential equations, *Comput. Math. Model.*, 23(1), pp. 96–106.
- [14] Kaushik A., (2014), Error estimates for a class of partial functional differential equation with small dissipation, *Appl. Math. Comput.*, 226, pp. 250–257.
- [15] Kuang Y., (1993), *Delay differential equations: with applications in population dynamics*, Academic press, New York.
- [16] Kumar D., Kumari P., (2019), A parameter-uniform numerical scheme for the parabolic singularly perturbed initial boundary value problems with large time delay, *J. Appl. Math. Comput.*, 59(1), pp. 179–206.
- [17] Mickens R. E., (1994), *Nonstandard finite difference models of differential equations*, World Scientific, Singapore.
- [18] Negero N. T., (2022), A uniformly convergent numerical scheme for two parameters singularly perturbed parabolic convection-diffusion problems with a large temporal lag, *Results Appl. Math.*, 16, 100338.
- [19] Negero N. T., (2023), A parameter-uniform efficient numerical scheme for singularly perturbed time-delay parabolic problems with two small parameters, *Partial Differ. Equ. Appl. Math.*, 7, 100518.
- [20] Negero N. T., (2023), Fitted cubic spline in tension difference scheme for two-parameter singularly perturbed delay parabolic partial differential equations, *Partial Differ. Equ. Appl. Math.*, 8, 100530.
- [21] Negero N. T., (2023), A fitted operator method of line scheme for solving two-parameter singularly perturbed parabolic convection-diffusion problems with time delay, *J. Math. Model.*, 11(2), pp. 395–410.
- [22] Negero N. T., Duressa G. F., (2022), Uniform convergent solution of singularly perturbed parabolic differential equations with general temporal-lag, *Iran. J. Sci. Technol. Trans. A Sci.*, 46(2), pp. 507–524.
- [23] Negero N. T., Duressa G. F., (2021), A method of line with improved accuracy for singularly perturbed parabolic convection-diffusion problems with large temporal lag, *Results Appl. Math.*, 11, 100174.
- [24] Negero N. T., Duressa G. F., (2022), An efficient numerical approach for singularly perturbed parabolic convection-diffusion problems with large time-lag, *J. Math. Model.*, 10(2), pp. 173–110.
- [25] Negero N. T., Duressa G. F., (2022), An exponentially fitted spline method for singularly perturbed parabolic convection-diffusion problems with large time delay, *Tamkang J. Math.*, <https://journals.math.tku.edu.tw/index.php/TKJM/article/view/3983>.
- [26] Negero N. T., Duressa G.F., (2022), Parameter-uniform robust scheme for singularly perturbed parabolic convection-diffusion problems with large time-lag, *Comput. Methods Differ. Equ.*, 10(4), pp. 954–968.
- [27] Podila P. C., Kumar K., (2020), A new stable finite difference scheme and its convergence for time-delayed singularly perturbed parabolic pdes, *J. Comput. Appl. Math.*, 39, pp. 1–16.
- [28] Sharma M., (2017), A robust numerical approach for singularly perturbed time delayed parabolic partial differential equations, *Differ. Equ. Dyn. Syst.*, 25(2), pp. 287–300.
- [29] Tesfaye S. K., Woldaregay M. M., Dinka T. G., Duressa G. F., (2022), Fitted computational method for solving singularly perturbed small time lag problem, *BMC Res. Notes*, 15(1), pp. 1–10.
- [30] Van Harten A., Schumacher J., (1978), On a class of partial functional differential equations arising in feed-back control theory, *North-Holland Math. Stud.*, 31, pp. 161–179.
- [31] Van Dyke M., (1994), Nineteenth-century roots of the boundary-layer idea, *Siam Review*, 36(3), pp. 415–424.
- [32] Woldaregay M. M., Aniley W. T., Duressa G. F., (2021), Novel numerical scheme for singularly perturbed time delay convection-diffusion equation, *Adv. Math. Phys.*, 2021, pp. 1–13.

- [33] Wu J., (2012), Theory and applications of partial functional differential equations, Vol. 119, Springer-Verlag, New York.



Naol Tufa Negero is an assistant professor of Mathematics at Wollega University, Nekemte, Ethiopia. He is the member of Department Committee at the College of Natural and Computational Sciences at Wollega University, Ethiopia.



Gemechis File Duressa is a Professor of Mathematics at Jimma University, Jimma, Ethiopia. Currently he is working as the director of the School of Graduate Studies at Jimma University.
